



Research article

Rational Formulation of targeted ABT-737 nanoparticles by self-assembled polypeptides and designed peptides

Polina Aibinder^a, Ifat Cohen-Erez^a, Hanna Rapaport^{a,b,*}^a Avram and Stella Goldstein-Goren Department of Biotechnology Engineering, Ben-Gurion University of the Negev, Beer-Sheva 8410501, Israel^b Ilse Katz Institute for Nanoscale Science and Technology (IKI), Ben-Gurion University of the Negev, Beer-Sheva 8410501, Israel

ARTICLE INFO

Keywords:

Apoptosis
BCL-2
β-sheet peptides
Self-assembly
Drug delivery
Cytotoxicity
Mitochondria
Nanoparticles

ABSTRACT

Here we present the development of nanoparticles (NPs) formulations specifically designed for targeting the antiapoptotic Bcl-2 proteins on the outer membrane of mitochondria with the drug agent ABT-737. The NPs which are self-assembled by the natural polypeptide poly gamma glutamic acid (YPGA) and a designed cationic and amphiphilic peptide (PFK) have been shown to target drugs toward mitochondria. In this study we systematically developed the formulation of such NPs loaded with the ABT-737 and demonstrated the cytotoxic effect of the best identified formulation on MDA-MB-231 cells. Our findings emphasize the critical role of solutions pH and the charged state of the components throughout the formulation process as well as the concentrations of the co-components and their mixing sequence, in achieving the most stable and effective cytotoxic formulation. Our study highlights the potential versatility of designed peptides in combination with biopolymers for improving drug delivery formulations and enhance their targeting abilities.

1. Introduction

The mitochondrial pathway of apoptosis is regulated by the B-cell lymphoma 2 (Bcl-2) family of pro- and antiapoptotic proteins. Overexpression of the antiapoptotic Bcl-2 proteins is linked to a downregulation of apoptosis. These proteins sequester the proapoptotic Bcl-2 homology 3 (BH3)-only proteins trigger apoptosis by either inactivating Bcl-2 or inducing an active conformation of Bax and Bak proteins that undergo oligomerization and generate the mitochondrial outer membrane permeabilization effect (MOMP) [1, 2]. BH3-mimetic drugs that promote Bax and Bak oligomerization [3–5], and the MOMP-induced apoptosis are considered an effective strategy for cancer therapy [6]. One such proapoptotic drug is ABT-737 which binds with a high affinity to the antiapoptotic Bcl-2, Bcl-xL, and Bcl-w proteins, that are located on the outer membrane of the mitochondria [7]. ABT-737 has shown a single-agent efficacy against tumor cells of multiple myeloma, acute myeloid leukemia, lymphoma, and solid tumor cell lines [8–10]. It has also shown activity in combination with standard therapies in leukemia and multiple myeloma models *in-vivo* [9,10]. Combinations of ABT-737 with the chemotherapy drug docetaxel or paclitaxel elicited synergistic therapeutic effects on the breast cancer cell lines [11, 12] MDA-MB-231 and MCF-7 and with doxorubicin or gemcitabine on thyroid carcinoma cells [13]. However, the therapeutic potential of ABT-737 has been limited by its low oral bioavailability and its poor aqueous solubility which hampers the potential utilization of the drug by intravenous delivery [14–16].

* Corresponding author. Avram and Stella Goldstein-Goren Department of Biotechnology Engineering, Ben-Gurion University of the Negev, Beer-Sheva 8410501, Israel.

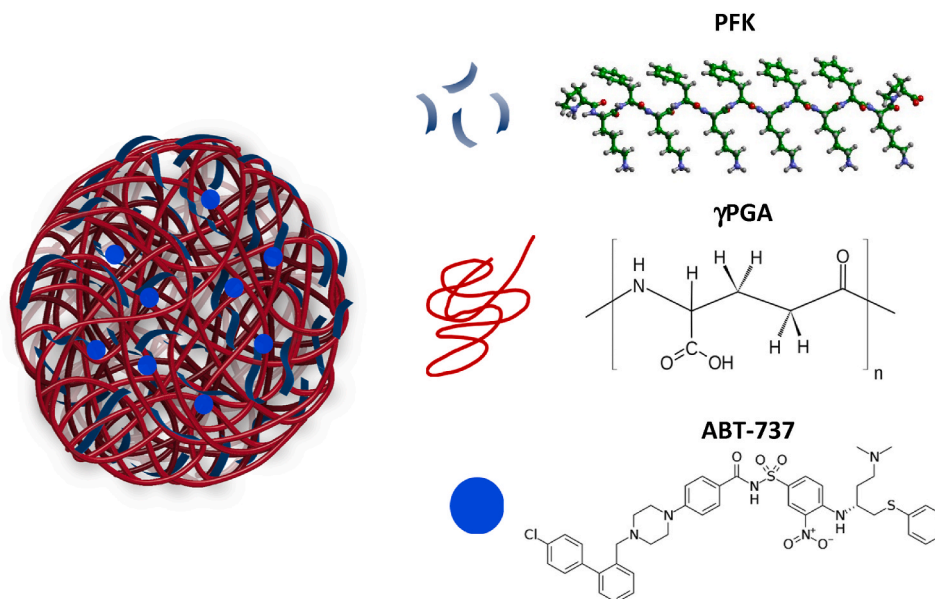
E-mail address: hannarap@bgu.ac.il (H. Rapaport).

<https://doi.org/10.1016/j.heliyon.2024.e26095>

Received 24 October 2023; Received in revised form 11 December 2023; Accepted 7 February 2024

Available online 8 February 2024

2405-8440/Â© 2024 Published by Elsevier Ltd. This is an open access article under the CC BY-NC-ND license (<http://creativecommons.org/licenses/by-nc-nd/4.0/>).



Scheme 1. Illustration of ABT-PoP-NPs (left) and its self-assembled components (right)..

In recent years, nanoparticles (NPs) have been used as solubilizing agents for improving drug bioavailability and targeting with lowering systemic toxicity [17,18]. NPs can specifically target cancer tissue by the enhanced permeability and retention (EPR) effect [19,20], that relies on the accumulation of NPs in the tumor tissue, due to lack of tight endothelial monolayer in tumor vessels [21–23]. Several NPs formulations have been reported to improve the potential therapeutic profile of ABT-737, including such that employed the hydrophobic polymer poly-lactic-co-glycolide acid (PLGA) which exhibited a half maximal inhibitory concentration, IC₅₀, of $8.9 \pm 1.0 \mu\text{M}$, with reduces thrombocytopenic effects in both *in-vitro* and *in-vivo* colorectal cancer models [24]. ABT-737 which was loaded onto PLGA-NPs coated with Notch-1 antibodies, exhibited an even lower IC₅₀ of 1.6 μM in cultures of MDA-MB-231 cells [25].

Peptides can be utilized to facilitate NPs' targeting to certain organelles within the cells [26–29]. Specifically, peptides consisting of positively charged and hydrophobic amino acids, play a significant role in overcoming membranous barriers of cells and mitochondria [30–32]. The group of Kelley developed mitochondria-penetrating peptides composed of alternating positively charged and hydrophobic residues that crossed the mitochondrial membranes [33]. Our group developed a mitochondria-targeted NPs system, that is based on a coassembly of two components, an anionic polypeptide with an amphiphilic and an oppositely charged designed peptide, denoted PoP-NPs [34–38]. Poly gamma glutamic acid (YPGA) is a biodegradable, non-toxic, non-immunogenic, biopolymer which has been shown to form NPs when combined with positively charged polymers. [39,40], The PoP-NPs are generated by a sequence of mixing steps that combine YPGA with the designed amphiphilic and cationic β -sheet peptide, Pro-Lys-(Phe-Lys)₅-Pro (PFK) [34]. PFK peptide, with its repeat of hydrophilic and hydrophobic amino acids, induces folding into β -sheet conformation and organizes into positively charged bilayer-fibrils under certain concentrations, pH, and electrostatic screening conditions [34–38,41]. The fibrils of PFK [42–45] in the NPs point their Phe side chains into the fibrils' interior, and their Lys residues to the surrounding anionic YPGA. The formulation of drug loaded PoP-NPs requires screening of various parameters along the process in order to optimize the performance of the system. We demonstrated that PoP-NPs, could be formulated with the anionic and hydrophobic small-molecule chemotherapeutic drug lonidamine (LND), to target the proximity of the mitochondria [26,30]. These LND-PoP-NPs led to tumor growth inhibition with no adverse side effects, upon intravenous administration in an MDA-MB-231 xenograft breast cancer murine model. The formulations of PoP-NPs were also adjusted to the IWP -2, a WNT inhibitor small molecule [37] and to the delivery of oligonucleotides [46].

Herein we demonstrate a rational formulation approach for enabling ABT-737 to be loaded onto PoP-NPs (Scheme 1) towards improving the drug's solubilization and cytotoxic effect. Various ABT-PoP-NPs formulations were designed and then characterized by their NPs size, zeta-potential and drug loading yield. The best developed formulation was tested for its cytotoxic effect on MDA-MB-231 cells.

2. Experimental section

2.1. Materials

PFK peptide, PK(FK)₅P, (MW = 1717 gr/mol) and PK(FK)₅P-FITC, PFK-FITC, were synthesized and then purified by high-performance liquid chromatography to 95% (GenScript, Piscataway, NJ). The polypeptide YPGA, 200–500 KDa, was purchased from Wako Chemicals (Tokyo, Japan). ABT-737 (purity >98%, MW = 813.43 gr/mol) was purchased from A2S Technologies (Yavne,

Israel). Unless otherwise specified, all reagents were purchased from Sigma-Aldrich (Rehovot, Israel) and were of the highest available purity. All solutions were prepared with deionized water (DIW) (18.2 MX cm, Direct Q-5 Merck Millipore, Billerica, MA).

2.2. Titration

Titration curves of ABT-737 were generated based on pH measurements performed at room temperature (CyberScan pH 510, Eutech Instruments, Thermo Scientific, Waltham, MA), versus added volume, V , of 0.01 M HCl. The first derivative of the titration curves, versus the titrant volume, dpH/dV , were utilized to determine the pK_a and equivalence values of the drug's ionizable groups. The titrated ABT-737 solution, 0.15 mg/mL, 0.5 mL, was prepared by diluting ABT-737 in DMSO solution (0.5 mg/mL, 0.61 mM) in DIW (30:70% v/v). This ABT-737 solution was supplemented with 5 μ L of 0.1 M NaOH to raise the pH to 9.5. The titration was conducted with 10 mL aliquots of the HCl solutions, accompanied by measurement of the pH, up to a total added volume of 770 mL, at which leveling to pH \sim 2.6 was noted. This pH was considered the lower limit of the pH meter. In addition, theoretical pK_a points were extracted from the program "Chemaxon" (<https://chemaxon.com/>) using the tool chemicalize.com.

2.3. Solutions and principal steps in NPs formulations

Each of the three components used for formulating ABT-PoP-NPs was first dissolved under specific conditions to generate the stock solutions that are then mixed in a certain order to facilitate the NPs' self-assembly. Either of two types of ABT-737 0.15 mg/mL aqueous solutions were used in the formulations. One stock solution of the drug, containing 30 % v/v DMSO in DIW, was prepared by mixing 0.3 mL of ABT-737 in DMSO solution, 0.5 mg/mL (0.61 mM) with 0.7 mL of DIW. The pH of this solution was adjusted to 3 by adding less than 20 μ L of 0.1 M HCl, followed by sonication for ensuring complete dissolution. The second ABT-737 stock solution at pH = 3, containing less than 1% v/v DMSO that was designated for cell-culture studies, was prepared by mixing 9 μ L of a concentrated (50 mg/mL, 61 mM) ABT-737 in DMSO solution, with 1 mL DIW, supplemented with <18 μ L of 0.5 M HCl and sonicated. PFK solutions, either 0.5 or 0.35 mg/mL, were prepared by dissolving the peptide powder in DIW followed by adjusting the pH to 7 with aliquots of 0.1 M NaOH. YPGA solutions were prepared at 0.5 mg/mL concentration by first, dissolving the polypeptide powder in 0.85 mL of 0.0023 M NaOH solution (pH \sim 11.5) followed by adjustment to pH \sim 7 and then complementing the volume to 1 mL with DIW. These solutions were next mixed together in different orders to identify the best performing PoP-NPs (all formulations are summarized in Table 1 and the main steps of the process are illustrated in Fig. 3 below). In the cases where turbidity appeared along the mixing steps, the solutions were clarified by centrifugation at 3000g for 20 min, followed by passing the supernatant through a syringe-driven 0.22 μ m filter (Merck Millipore, Millex GV 0.22 μ m, Billerica, Massachusetts, USA). Finally, formulated PoP-NPs solutions were either characterized as is or were first subjected to a concentration step using a vacuum evaporator, operated at 30 °C (CentriVap DNA Vacuum Concentrator, Labconco, Kansas City, Missouri, USA), or centrifugal filtration (Vivaspin ® 20, 100 kDa, Sartorius Stedim Lab Ltd. UK) that is followed by recovering the unfiltered solution. These solutions were concentrated in order to achieve drug concentrations that are approximately X20 compared to the previously reported IC50 values [24,25] in order to enable their effective dilution into the cell culture media in the cells' viability studies. ABT-737 concentration in the various solutions was determined by OD measurements at 310 nm using a spectrophotometer (Multiskan Go, Thermo scientific, MA) and a calibration curve. ABT-737 yield in ABT-PoP-NPs solutions was calculated using the concentration of the drug applied in preparing the NPs, and its concentration in the finally formulated NPs solutions.

2.4. NPs size and charge

NPs hydrodynamic radius was measured by dynamic light scattering (DLS) (CGS-3 LSE-5003, ALV, Langen, Germany) applying the detector at a 90° angle. Zeta potential of NPs was measured by a zetasizer (Nano ZS, Malvern, Worcestershire, UK), and data were analyzed using the Smoluchowski model, provided as part of the instrument's analysis computational package.

2.5. Atomic force microscopy (AFM)

The NPs were imaged by atomic force microscopy (MFP-3D-Bio, Asylum Research/Oxford Instruments) using AC40 probes (Olympus, Japan) in an AC-mode in aqueous phase, on a mica substrate. A 10 μ L drop of each ABT-PoP-NP and PoP-NP solutions was placed on a freshly cleaved mica and the deposited drop was maintained for \sim 4 min (while preventing it from drying) to allow adsorption of the NPs onto the mica surface. Next, 100 μ L DIW were added on top of the drop, after which the scan was initiated.

2.6. Thermal gravimetric analysis (TGA)

TGA analysis in combination with OD measurements were used to determine the weight percentage of the drug in ABT-PoP-NPs (formulation A5.1 described in the Results section). The thermogravimetric analysis was used to determine the total organic content in the NPs and the OD measurement was used to specifically determine the concentration of the ABT-737 in the solution subjected to vacuum evaporation. The two values specify the weight percentage, % w/w, of ABT-737 in the ABT-PoP-NPs.

For the TGA measurement the ABT-PoP-NPs formulation A5.1 was prepared in an 18 mL scale. Three mL of ABT-737, 0.15 mg/mL (<1% DMSO) at pH = 3 was mixed with 3 mL YPGA 0.5 mg/mL solution. The mixture was diluted by 9 mL DIW (all other details as described above in NPs formulation). This 15 mL solution was titrated to pH \sim 7.4 and stirred for 1 h by a magnetic stirrer, at room

temperature. The solution was mixed with 3 mL PFK for 1 h to provide the ABT-PoP-NPs solution. In addition, for a reference, the solutions of YPGA and PFK were prepared the same way as for the ABT-PoP-NPs and diluted with DIW to 18 mL, to obtain same concentrations as in the NPs solution. The solutions of ABT-PoP-NPs, and for a reference also the YPGA, PFK and ABT-737 solutions, were dried down to a volume of 2 mL at which OD measurements were performed. Next, these solutions were completely dried overnight under vacuum. Each of the obtained powders was weighted and then a certain weight was subjected to the TGA measurement (TGA, TA Instruments Q500, New Castle, DE), while flushed by nitrogen, at a flow rate of 90 mL/min and heated at 10 °C/min to 1000 °C. TGA provided the organic content, i.e. the total weight of ABT-PoP-NPs (including the free peptide, drug and poly-peptide in the NPs solution). Using the drug concentration value as obtained by the OD measurements and the organic content of the ABT-PoP-NPs dry weight, the drug's w/w % can be calculated using the following formula (1):

$$\text{ABT-737 in ABT-PoP-NPs (w/w\%)} = \left(W_{TGA} * W_{SpV}^{ABT} \right) / \left(W_{SpV} * W_{TGA}^{organic} \right) \times 100 \quad (1)$$

W_{TGA} - weight of the ABT-PoP-NPs dry powder subjected to the TGA

W_{SpV}^{ABT} - weight of ABT-737 calculated based on ABT-737 concentration as measured by OD in the 2 mL ABT-PoP-NPs concentrated solution, that was obtained by drying under vacuum.

W_{SpV} - weight of the dry ABT-PoP-NPs powder, obtained after the vacuum drying.

$W_{TGA}^{organic}$ - weight of organic material determined as the weight loss during TGA at 120–600 °C.

NPs concentration (excluding residual water and salts) in mg/ml, was calculated by formula (2):

$$\left(W_{SpV} * W_{TGA}^{organic} \right) / \left(W_{TGA} * V_{SpV} \right), \text{ where:} \quad (2)$$

V_{SpV} - volume, 2 mL, of concentrated ABT-PoP-NPs used in this measurement

2.7. Cell viability studies

The effect of ABT-PoP-NPs on cell viability was tested with the same formulation that was described above in the TGA analysis but with all solutions undergoing 2 min sonication (Sonics Vibra-cell VCX-130 sonicator, Newtown, CT, USA) at 45 % amplitude, and with the final NPs solution concentrated by centrifugal filtration (denoted formulation A5.2). This concentrated solution was sterilized by UV light for 30 min prior to its application. The cytotoxicity of the ABT-PoP-NPs was assessed with MDA-MB-231 cells (ATCC) in 96-well plates, 5×10^3 cells/well, seeded in 150 μ L DMEM complete medium and cultured overnight. The cells were supplemented with 50 μ L of different concentrations of ABT-PoP-NPs or control PoP-NPs (prepared as formulation A5.2 but with 3 mL DIW, deprived of the drug), while the final concentrations of ABT-737 were: 5, 10, 20, 30, 40, 50 μ M and NPs concentrations: 0.03, 0.05, 0.11, 0.16, 0.22, 0.27 mg/mL. The cell were cultured over three days. Cell viability was determined by XTT assay following the manufacturer's instructions (Biological Industries Israel Beit-Haemek). The medium was replaced and XTT solution was added to the cultured cells and incubated for 2 h after which the OD at 490 nm was measured by a microplate-reader (BioTek instruments, Winoosky, VT). Cell viability is reported as a percentage compared to untreated cultured cells.

Caspase 3 activity in the MDA-MB-231 cells was determined using the caspase 3 assay kit (ab39383, Abcam, Cambridge, UK) according to the manufacturer's protocol. Briefly, cells were seeded in 6-well plate, 3×10^5 cells/well in 3 mL DMEM complete medium and cultured overnight. Each well was supplemented with 1 mL PoP-NPs, ABT-PoP-NPs to obtain a final concentration of 30 μ M of the drug (close to IC50 measured herein, see Results Section) or saline, and cultured overnight. After the incubation, the cells were rinsed with PBS, lifted of the plate with trypsin and resuspended in chilled PBS to yield a cell suspension that was centrifuged at 4 °C. The cells were counted, and 200,000 cells were lysed by lysis buffer, added to the fluorogenic substrate DEVD-AFC (AFC: 7-amino-4-trifluoromethyl coumarin) and incubated at 37 °C for 2 h. The fluorescence (excitation/emission = 400/505 nm) was measured by plate reader (Biotek, Winooski, VT, USA) in duplicates. Caspase activity levels were represented as a normalized ratio compared to the untreated saline supplemented cells.

The visualization of cellular uptake was performed with ABT-PoP-NPs that were prepared as described above, but with 30 % weight of the peptide replaced by PFK-FITC. MDA-MB-231 cells (3×10^5 cells/well) were cultured overnight in a confocal dish (μ -Dish 35 mm, high, ibidi, Germany) with DMEM complete medium. Then the medium was replaced with a fresh medium containing MitoTracker Red (MitoTracker Red CMXRos, Thermo Fisher) at a final concentration of 100 nM, and the cells were incubated for 40 min to allow the mitochondria to be stained. Cells were then washed with PBS, and the medium was replaced with fresh phenol red free medium and observed by a confocal microscope with super resolution (140 nm) and a spectral imaging (Zeiss LSM880 Airyscan, Germany).

3. Results and discussion

3.1. Titration curve of ABT-737

The PoP-NPs formulation is strongly influenced by the charged state of its co-assembled components. The two main components of PoP-NPs are oppositely charged at neutral pH according to the pK values of their charged groups; the carboxyls of YPGA and the Lys groups of PFK that are characterized by $pK_a = 4.25$ and 10.53 respectively [47]. To identify the pKa values of ABT-737, we first utilized a molecular modeling calculator (Chemaxon's tools, [chemicalize.com](https://www.chemicalize.com)). The program identified four charged groups for ABT-737 with

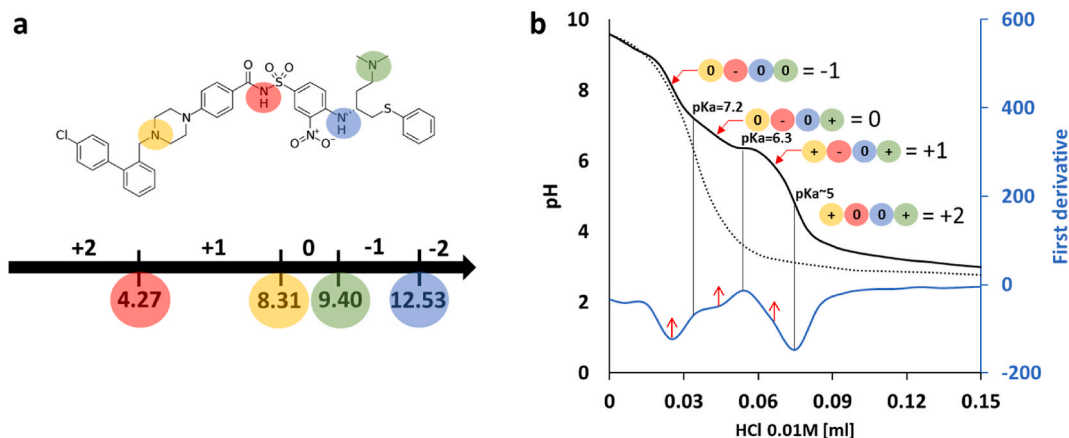


Fig. 1. The charge states of ABT-737 as a function of pH. (a) The theoretical pKa values of ABT-737 attributed to the charged groups that are highlighted in color in the molecular structure (top) and the pKa values, identified by Chemicalize tool on www.chemaxon.com, presented schematically along an arrow with the net charge of the molecule (bottom). (b) Titration curve of ABT-737 0.15 mg/mL in 30 % v/v DMSO:DIW solution (black line), first derivative (dpH/dV, blue line) used for identifying pKa and equivalence points marked by vertical lines and red arrows, respectively. For a reference a titration curve of NaOH aqueous solution (grey dotted line) is presented.

the pKa values: 4.27, 8.31, 9.40, and 12.53, attributed to the sulfonamide, piperazine-amine, the tertiary amine, and the secondary amine respectively (Fig. 1a). Next, we attempted to monitor the pKa values of ABT-737 using a titration curve (Fig. 1b). A solution of ABT-737, 0.15 mg/mL, was prepared by diluting the drug in DMSO stock solution into DIW, generating a 1 mL drug suspended in 30 % v/v DMSO in DIW. This solution was adjusted by aliquoted of 0.1 M NaOH to pH = 9.5 and the titration was performed by 0.01 M HCl. A first order derivative of the titration curve (dpH/dV, Fig. 1b) was generated to assist in identifying deflection points in the titration curve. These were attributed to pKa points, each followed by an equivalence state. In this manner three pKa values were identified, at pH = 7.2, 6.3 and ~5.0. These pKa values may correspond to the theoretically calculated values of 9.4, 8.31 and 4.27, respectively but with a large deviation from the theoretically calculated values, possibly due to the DMSO's effect on the drug's protonation states [48, 49]. Nonetheless, based on the experimentally detected pKa values and backed by those calculated, the different charged states of the ABT-737 solution, as a function of pH, could be delineated (Fig. 1b). At pH higher than the theoretically assigned pKa = 12.5 point, the overall charge of ABT-737 is expected to be -2. Then upon crossing this pH and down to pH < 7.2 the secondary and tertiary amines should become protonated, turning the ABT-737 into a neutrally charged molecule. At the pH values of 6.3 and then below ~5 the piperazine and the sulfoamide groups, may become protonated [50] turning the charge of ABT-737 to +1 or +2, respectively. Zeta potential measurements for the 0.15 mg/mL ABT-737 in 30 %v/v DMSO solution corroborated a net positive charge, +31 mV, at pH = 3.0 and a net negative charge, -25.6 and -52.4, at pH = 7 and 11, respectively. Of note, based on naked eye observation, the net negative charge at pH > 7.2 is found to be less effective than the net positive charge at pH ~3, in dissolving the drug. Hence the formulations of the NPs were conducted with the ABT-737 stock solutions at pH = 3.

3.2. Formulation of ABT-PoP-NPs

The formulation of ABT-PoP-NPs was first based on the protocol we previously developed, for LND-loaded PoP-NPs [35]. The co-assembly process of LND-PoP-NPs uses stock solutions of the drug, PFK and the YPGA, each dissolved in aqueous solutions, at concentrations 0.15, 0.5 and 0.5 mg/mL respectively, that are mixed in a certain order [35]. For the ABT-737 formulation a solution of the drug at 0.15 mg/mL, was prepared as described above, in 30 %v/v DMSO in DIW solution adjusted to pH = 3. Next, one mL of this ABT-737 solution was mixed with an equal volume of 0.5 mg/mL PFK dissolved in DIW (pH ~ 5). Although the two compounds are positively charged at this range of pH values, and therefore were not expected to interact, a mild opacity in the mixed solution was observed (Fig. 2a) indicative of the drug precipitation. Next, this 2 mL ABT-737:PFK suspension, was supplemented with 1 mL of the 0.5 mg/mL YPGA and the mixture was adjusted to pH = 7.4, to allow the three components to possibly reorganize into NPs over this time course. Nonetheless, the turbidity of the three components mixture (Fig. 2b) appeared enhanced compared to the ABT-737:PFK mixture, and it remained so after the one day stirring. Of note, this mixture is characterized by an excess of anions according to the concentrations of the three components: 0.05, 0.17 and 0.17 mg/mL of ABT-737, PFK and YPGA, respectively and their corresponding net charges: 0.12, 0.58 mmol/mL of cations (considering +2 and + 6 charges per ABT-737 and PFK molecules, respectively) and 1.13 mmol/mL anions (assuming each monomer of YPGA carries a -1 charge) and apparently this factor was not sufficient in turning the system into NPs. This suspension was next centrifuged to remove aggregates (clusters of material that are visible to naked eye) and then the supernatant was passed through a 0.22 μ m syringe filter to yield an apparently clear solution, which was further characterized to detect the presence of NPs (Fig. 2c). This formulation, denoted A1, was analyzed by DLS, zetasizer and by OD (310 nm) measurements, to determine hydrodynamic diameter, surface charge and ABT-737 concentration of potentially present NPs. These measurements indicated the presence of NPs with a radius = 11.2 ± 5.17 nm and a zeta potential equal to -35.1 ± 2.52 mV, but with a low

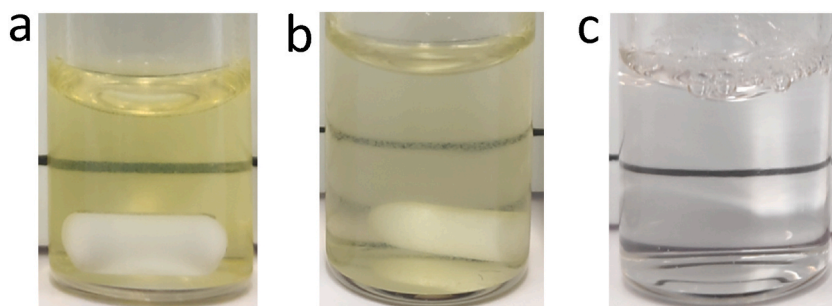


Fig. 2. Representative images of stages along the A1 formulation. Glass vials are positioned in front of paper with a black line to demonstrate the turbidity or clarity of the mixtures. (a) The two-component ABT-737 and PFK mixture showing turbidity despite the mixing by a magnetic stirrer. The drug provides the yellow color. (b) The three-components mixture of ABT-737, PFK and γ -PGA, after adjusting the solution to pH = 7.4. (c) This three components solution following centrifugation and filtration through a 0.22 μ m filter, appearing clear but also absent of the yellowish color that characterizes the drug.

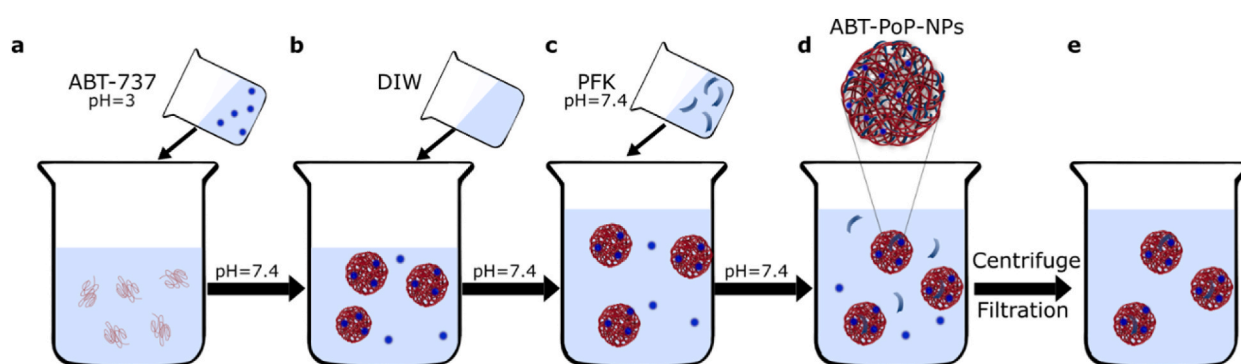


Fig. 3. Schematic description of ABT-PoP-NPs, A2-A5, formulations. (a) An aqueous solution of the negatively charged YPGA is mixed under stirring with ABT-737 which is positively charged at pH = 3. (b) DIW is added to the two components solution according to the specific formulation detailed in Table 1. (c) PFK solution at pH = 7.4 is added. Each of the steps is followed by adjustment of the obtained solution to pH = 7.4. The three components co-assemble into (d) the ABT-PoP-NPs and free components (e) ABT-PoP-NPs solution after the centrifugation and filtration was found to contain 1.4 %w/w of free components (Supplementary, Table S2).

concentration of the drug 0.0028 ± 0.0019 mg/mL that corresponds to a low yield of only 5 ± 3.75 % of the formulation. This low drug yield of A1 formulation, prompted us to explore different assembly routes.

The formulation of ABT-PoP-NPs was next modified, so to first create favorable electrostatic interactions between the cationic ABT-737 drug and the anionic YPGA, in the same mole excess of the anionic groups as indicated above. This was followed by the addition of the cationic PFK solution to the mixture. Specifically, one mL of ABT-737, 0.15 mg/mL dissolved in DMSO = 30 %v/v, pH = 3, was added dropwise under a continuous stirring, to a one mL YPGA 0.5 mg/mL, and the mixture was adjusted to pH 7.4 using aliquots of 0.1 M NaOH. This ABT-737:YPGA solution, containing 0.18 and 1.7 mmol/mL of cations and anions respectively, was clear to the naked eye (Fig. 3, step a). Next, in order to reduce potential aggregation that may occur upon the subsequent addition of the peptide, this 2 mL ABT-737:YPGA solution was first diluted by 1 mL DIW (Fig. 3, step b) and then supplemented by a one mL of either 0.5 or 0.35 mg/mL PFK, to yield the ABT-PoP-NPs formulations denoted A2 and A3, respectively. The mildly turbid solutions of A2 and A3 that were centrifuged and passed through a filter as described above, exhibited a drug yield of 12.3 ± 3.4 % and 37.6 ± 5.5 % both higher than that of A1 formulation. Interestingly, the lower concentration (0.35 mg/mL) PFK solution used in formulation A3 (Table 1), resulted in a higher drug yield compared to A2, possibly due to reducing the chances for aggregation. Hence the 0.35 mg/mL PFK solution was further applied in the formulations described below.

In an attempt to further reduce aggregation, that was evident by the mild turbidity that appeared following the addition of the peptide to the ABT-737:YPGA solution, a larger dilution of DIW, of 2 or 3 mL, was utilized (Fig. 3, step b) generating formulations denoted A4 and A5 respectively (Table 1). Following the centrifugation and filtration steps, A4 and A5 solutions showed NPs of 13.8 ± 4.2 and 10.3 ± 1.6 nm in radius, both with a negative zeta potential and with an improved drug yield of 45 ± 3.9 and 49.2 ± 4.2 %, respectively (Table 1) corresponding to 12–14 μ M of the drug. These results indicated that the dilution step (Fig. 3, step b) helped in lowering non-specific aggregation. In an analysis of formulation A5.2 described in supplementary it was found that 1.4 w/w% of all the organic matter remained free in the solution, hence the drug yield values represent well the encapsulation efficiency of the drug. To corroborate the presence of ABT-PoP-NPs in formulation A5, a 10 μ L of this solution was placed on a mica surface and scanned by atomic force microscopy (AFM). The scanned image showed mostly well separated NPs, with a near spherical shape, 2–3 nm in height and ~ 6 nm in diameter (Fig. 4a). The superiority of ABT-PoP-NPs in maintaining the drug soluble at physiological pH compared to the

Table 1
Characteristic properties of ABT-PoP-NPs A3-A7 formulations.

Formulation	pH	Dilution [mL] ^a	Radius [nm] ^b	ZP [mV]	ABT-737 [μ M]	Yield% of ABT-737
A3	7.4	1	8.2 \pm 1.9	-40.8 \pm 0.9	13.8 \pm 2.0	37.6 \pm 5.5
A4	7.4	2	13.8 \pm 4.2	-34.3 \pm 3.4	13.3 \pm 2.0	45.3 \pm 3.9
A5	7.4	3	10.3 \pm 1.6	-35.7 \pm 1.2	12.1 \pm 1.0	49.2 \pm 4.2
A5.1 ^c	7.4	3	10.9 \pm 4.2	-46.1 \pm 1.5	80.1 \pm 7.8	-
A5.2	7.4	3	9.3 \pm 1.8	-61.6 \pm 0.3	200 ^d	-
A6	8	2	15.2 \pm 6.3	-36.2 \pm 0.2	13.1 \pm 1.0	52.6 \pm 4.0
		3	14.8 \pm 5.1	-35.4 \pm 1.6	11.7 \pm 1.1	62.8 \pm 5.7
A7	9	2	10.4 \pm 1.8	-43.8 \pm 1.8	1.3 \pm 0.2	5.04 \pm 0.66
		3	13.2 \pm 2.6	-39.5 \pm 0.9	1.8 \pm 0.4	9.8 \pm 1.9

^a The indicated dilution refers to formulation prepared using one mL of the drug solution with one mL g-PGA, which is further supplemented with one mL of 0.35 mg/mL PFK solution.

^b The radii, zeta potentials, drug yields and final drug concentrations as measured following centrifugation and filtration. A6-7 formulations were adjusted to the detailed final pH values.

^c Formulations A5.1 and A5.2 were prepared the same way as A5 but with the drug stock solution that provides <1% v/v DMSO in the final formulation. A5.1 was concentrated by vacuum evaporation and A5.2 was concentrated by centrifugal filtration. The stability of A5.1 formulation at 4 °C was examined for 10 days (Supplementary Table S3). N = 3.

^d Solution concentrated was adjusted according to OD measurements to 200 μ M.

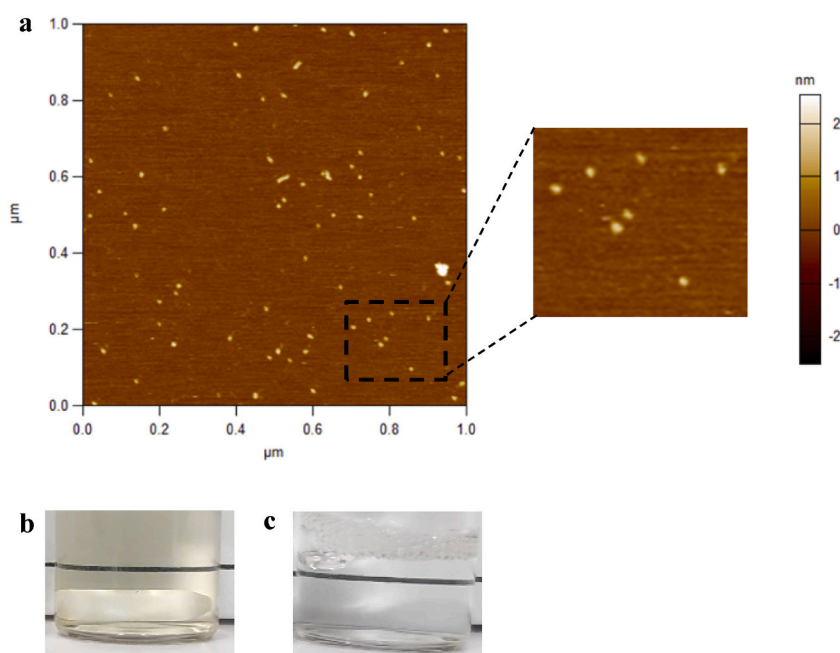


Fig. 4. (a) AFM of ABT-PoP-NPs, formulation A5 (see Supplementary for formulations A4 and A6); (b–c) ABT-737 free drug in 30% v/v DMSO:DIW solution adjusted to pH = 7.4, before (b) and after (c) filtration. The images demonstrate that upon pH adjustment the drug formed aggregates, that did not pass the 200 μ m filter, as evident by the loss of the drug's yellowish color in the filtered solution.

free drug stock solution was demonstrated with the 0.15 mg/mL, pH = 3 in 30 %v/v DMSO:DIW solution that was adjusted to pH = 7.4 by aliquots of NaOH. The free drug solution turned immediately opaque and a mild aggregation could be noted by naked eye. Following centrifugation and filtration the solution turned clear but with no evidence to the yellowish color of the drug (Fig. 4c). OD measurements indicated that only 0.31 μ M of the drug remained in this tested solution whereas the rest 98.6 % of the drug aggregated. This test demonstrates that the ABT-PoP-NPs formulation, for example that of A5, improves by a factor of almost x40 (12.1/0.31) the potential availability of ABT-737 drug under a physiological pH.

Two formulations denoted A5.1 and A5.2 were prepared towards cell culture experiments, using the same procedure as that of A5 but with the more concentrated solution of the drug in DMSO (50 mg/mL, see Experimental), that provides <1% v/v DMSO in the final ABT-PoP-NPs solution. A5.1 formulation was concentrated by a vacuum concentrator operated for 12 h that was found to not alter the hydrodynamic radius of the ABT-PoP-NPs, 10.9 \pm 4.2 nm, compared to the A5 solution (Table 1). This concentrated solution contained 80.1 \pm 7.8 mM of ABT-737, according to OD measurements. Next, formulation A5.2 was prepared with all the three stock solutions sonicated prior to their mixing with the other components, and the resultant NPs solution concentrated by a centrifugal filtration.

Interestingly this A5.2 showed ABT-PoP-NPs with a radii, 9.3 ± 1.8 nm and a more negatively charged zeta potential of -61.6 ± 0.3 mV. The concentration of A5.2 by centrifugal filtration was faster compared to the vacuum evaporation, and provided the ABT-PoP-NPs with the highest achieved drug concentration of 200 μ M. Of note, the filtrate of A5.2 solution was found to contain <1.4 % w/w of organic matter (Supplementary, Table S2) indicating that the centrifugation and filtration steps are efficiently removing free organic matter that is not self-assembled within the PoP-NPs. Following UV sterilization A5.2 was utilized in the cell culture studies described below.

Additional formulations based on that of A5 were tested in which the final pH was adjusted to values higher than physiological, aiming to improve the NPs stability and solubility. These formulations were prepared with the ABT-737:YPGA mixtures diluted by either 2 or 3 mL DIW, followed by the addition of one mL PFK, 0.35 mg/mL, and then adjusted with aliquots of 0.5 M NaOH to either pH 8 or 9 (denoted formulations A6 and A7, respectively; see Table 1). There were no large differences observed between the 2 and the 3 mL dilutions with respect to the NPs size and their zeta potentials. Formulation A6 showed size and zeta potential similar to those obtained for formulations A4 and A5 but with a higher drug yield, 52.6 and 62.8 % for the 2 and the 3 mL dilutions, respectively. However, formulation A7 (pH = 9) that was evidently more turbid than the previously tested A3-A6 formulations showed low values of drug yield. Hence, it may be concluded that at pH = 9 the favorable electrostatic interactions between the ABT-PoP-NPs components are lost, possibly due to the negative charge ABT-737 may acquire at this pH and the tendency of PFK to lose its charge at around this pH value. Despite the improved drug yield of formulation A6, due to fact that it entails a pH higher than that of physiological, NPs' characterizations and cell culture assays were performed with the A5 formulations.

3.3. TGA characterization of ABT-PoP-NPs

TGA thermograms of the ABT-PoP-NPs A5.1 formulation, and the pure components for a reference were measured to determine the w/w % of ABT-737 relative to ABT-PoP-NPs' organic matter. To obtain enough of the ABT-PoP-NPs for the TGA measurements the formulation of A5.1 (Table 1) was performed on an 18 mL scale, that was subsequently concentrated by evaporation under vacuum. The four TGA thermograms (Fig. 5) started with a weight loss in the 25–120 °C range, that is associated with water evaporation. This was followed by the 120–600 °C range in which organic matter decomposes, and that above 600 °C which is related to inorganic salts' evaporation. Applying a first derivative calculation to the TGA thermogram, peaks that represent shift in the evaporating phase could be identified. The free ABT-737 showed peaks at 281 and 330 °C possibly related to different aggregation forms. Similarly different aggregation forms of PFK resulted in first derivative peaks at 226, 299 and 343 °C and that of YPGA showed peaks at 263 and 349 °C. ABT-PoP-NPs exhibited two unique first derivative peaks, at 253 and 318 °C suggesting that the specific formulation steps that are relying on electrostatic interactions between its organic components is reflected in the NPs' unique TGA pattern. Based on these measurements the total organic concentration in the 18 mL ABT-PoP-NPs solution was found to be 0.052 ± 0.007 mg/mL. This value matches well the total organic concentration, 0.048 mg/mL, as expected based on the starting solutions used for the NPs formulation while excluding the salt content of each of the components and accounting for the yield following centrifugation and filtration (see Table S1). Next, the ABT-737 content in the ABT-737 powder applied for the TGA analysis was extracted from the OD measurements of the original ABT-PoP-NPs solution. Furthermore, the ABT-737 wt relative to the total organic weight comprising the ABT-PoP-NPs (extracted from the TGA see Supplementary) was calculated to be 14.1 ± 1.8 % w/w. This value corresponds well with the theoretical ratio between the ABT-737 concentration 0.15 mg/mL and the total organic concentration, 1 mg/mL, used in the formulations.

3.4. The cytotoxic effect of ABT-PoP-NPs

The cytotoxic effect of ABT-PoP-NPs, formulation A5.2, on MDA-MB-231 cell line was evaluated by the XTT viability assay, in cultures incubated for three days with different concentrations of the NPs treatment. A significant decrease in cell viability was observed in cells treated with the ABT-PoP-NPs compared to non-treated cells (Fig. 6a) with an $IC_{50} = 27.5 \pm 0.8$ μ M. Cells that were

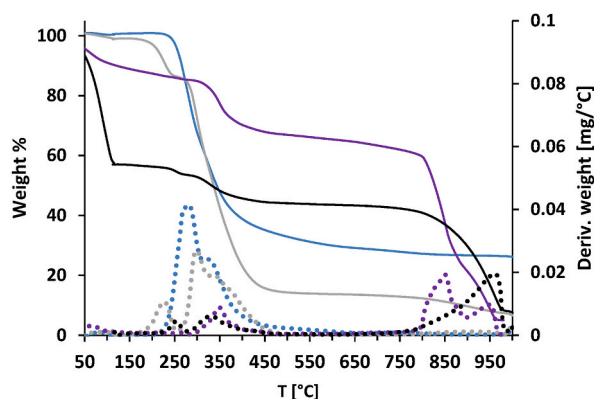


Fig. 5. TGA curves showing the weight % loss during the heating (continuous lines) and the Derivative of weight versus temperature [mg/°C] (dotted lines) of ABT-737 (blue), PFK (grey), YPGA (purple) and ABT-PoP-NPs (black).

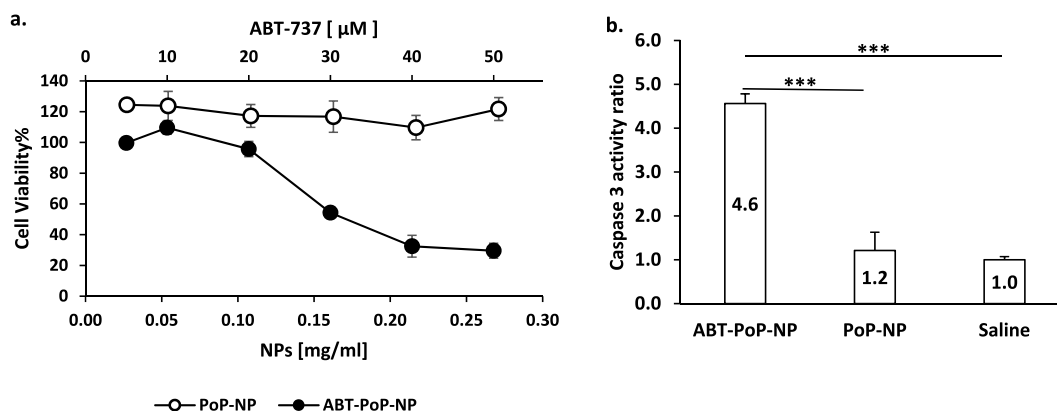


Fig. 6. (a) Viability of MDA-MB-231 cell line following a three days incubation in the presence of ABT-PoP-NPs and control of PoP-NPs at different concentrations. The drug concentration in ABT-PoP-NPs is provided in the upper axis. Cells' viability was normalized to untreated group; for the effect of a free drug solution, appearing aggregated on the cells' viability, see Fig. S3 N = 3. Of note, viability of the PoP-NPs treated cells reaches more than 100% viability possibly due to enrichment of the medium by the NPs components. (b) Caspase 3 activity measured in MDA-MB-231 cells following treatment with ABT-PoP-NPs and compared to PoP-NPs, all normalized to cells supplemented with saline and compared by independent sample t tests *P < 0.05, **P < 0.01, and ***P < 0.001. N = 3.

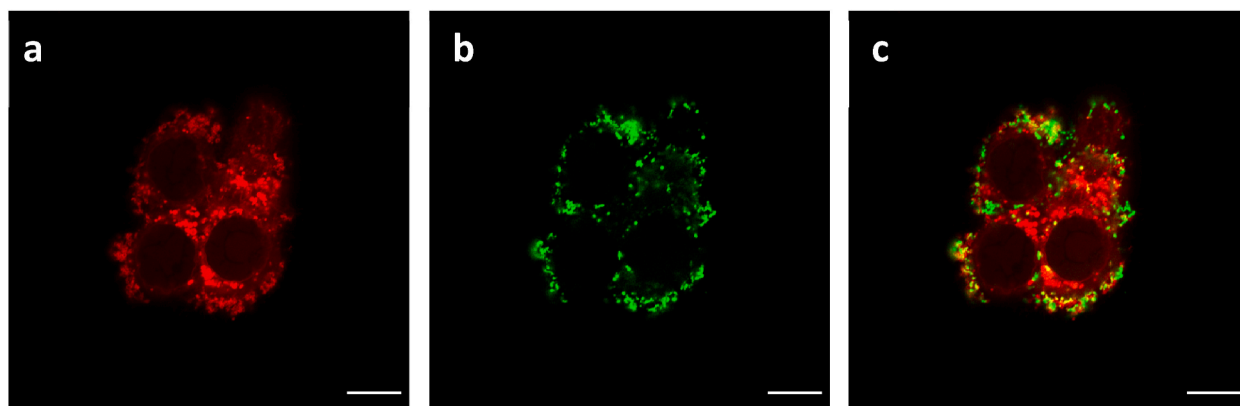


Fig. 7. Intracellular confocal images of ABT-PoP-NP incubated with MDA-MB-231 cells (bar = 10 μ m). Mitochondria were stained with MitoTracker Red (red color), shown in (a). ABT-PoP-NPs were labeled with PFK-FITC (green color), shown in (b) and ABT-PoP-NPs colocalized with mitochondria are detected as yellow color spots in the merged image (c).

treated for a reference with the PoP-NPs version (drug deprived formulation) showed a small increase in viability compared to the non-treated cell culture (see Fig. 6 legend), indicating that the ABT-PoP-NPs cytotoxic effect is induced by the drug. This IC₅₀ value of the ABT-PoP-NPs is only one order of magnitude larger compared to previously reported ABT-737 NPs, which were based on enhanced PLGA formulations containing either an additional cytotoxic drug [24] or a targeting antibody [25]. Also, the group treated with the ABT-PoP-NPs showed a smaller confluency compared to cells without treatment (see Supplementary Fig. S2). Due to the tendency of the free drug solution to quickly precipitate under physiological pH the cytotoxic effect of the free drug could not be reliably determined (see Supplementary Fig. S3).

In order to assess the effect of ABT-737 on cellular apoptosis, caspase 3 activity was measured in MDA-MB-231 cells (Fig. 6b). The increase in caspase 3 activities was significant after the treatment with ABT-PoP-NPs as compared to the drug-free PoP-NPs that had no effect compared to untreated cells. These results indicate that ABT-PoP-NPs induce cell apoptosis.

The cellular uptake of ABT-PoP-NPs and their colocalization within the proximity of mitochondria were evaluated by confocal microscopy (Fig. 7). MDA-MB-231 cells were incubated overnight with fluorescently labeled ABT-PoP-NPs (see Experimental) and mitochondria were then stained with Mito Tracker Red. The ABT-PoP-NPs (green stained, Fig. 7b) colocalized with stained mitochondria (Fig. 7a) appear as yellow clusters in the merged image (Fig. 7c). Based on image analysis, the average co-localization percent of NPs and mitochondria versus total NPs was found to be 21.2 ± 6.1 %. This analysis provides visual confirmation for the internalization of ABT-PoP-NPs into the cells and to their ability to co-localize with mitochondria.

4. Conclusions

This study demonstrates that the PoP-NPs co-assembly platform, with its oppositely charged components, the anionic polypeptide, YPGA, and the cationic and amphiphilic peptide PFK, can be efficiently formulated to carry the antiapoptotic ABT-737 drug. The PoP-NPs platform features significant advantages, primarily characterized by its precise control over the formulation process, that exclusively employs aqueous solutions, and straightforward stirring techniques. In our previous research, we successfully demonstrated the encapsulation of an anionic drug (LND) within PoP-NPs. In this current study, we present a comprehensive guide for the encapsulating of cationic drugs such as ABT-737, onto this platform. The ABT-PoP-NPs can be efficiently formulated within a few hours and readily employed in the investigation of its impact on various in-vitro cell models. Our findings emphasize the critical role of solutions pH and the charged state of the components throughout the formulation process, the concentrations of the components and their mixing sequence, in achieving the most stable and effective cytotoxic formulation. Based on the various formulations explored herein, it can be concluded that the first assembly step by electrostatic interactions, between YPGA and the oppositely charged ABT-737, plays a significant role in stabilizing the final formulation of the ABT-PoP-NPs. The formulation showed an optimal drug yield at near neutral pH that is preferable for cell culture studies and future applications of this NPs platform. The stable solution of ABT-PoP-NPs A5.2 formulation showed cytotoxicity towards MDA-MB-231 breast cancer cell line at drug concentrations in the micromolar range pointing to the effective release of the drug within the cells. Indeed, the ABT-PoP-NPs could be tracked by for colocalization with mitochondria by confocal microscopy. This study demonstrates the systematic development of NPs formulations based on intermolecular interactions that could be useful for future development of similar self-assembly systems for drug delivery.

Notes

The authors declare no competing financial interest.

Data availability statement

Data included in article/supp. Material/referenced in article.

CRedit authorship contribution statement

Polina Aibinder: Writing – original draft, Methodology, Investigation, Formal analysis, Data curation. **Ifat Cohen-Erez:** Writing – original draft, Formal analysis. **Hanna Rapaport:** Writing – review & editing, Methodology, Funding acquisition, Conceptualization.

Declaration of competing interest

The authors declare that they have no known competing financial interests or personal relationships that could have appeared to influence the work reported in this paper.

Acknowledgments

P.A. thanks the Feiffer family for the Ph.D. fellowship in the field of Bio-nanotechnology towards improving anticancer treatments. We thank the Avram and Stella Goldstein-Goren fund for support. Thanks to IKI members: Dr. Juergen Jopp for assisting with AFM measurements, Dr. Milionshchik Anna for the support in TGA measurements and Dr. Sharon Hazan for help with DLS and ZP measurements.

Appendix A. Supplementary data

Supplementary data to this article can be found online at <https://doi.org/10.1016/j.heliyon.2024.e26095>.

References

- [1] J. Kale, E.J. Osterlund, D.W. Andrews, BCL-2 family proteins: changing partners in the dance towards death, in: *Cell Death and Differentiation*, vol. 25, Nature Publishing Group, 2018, pp. 65–80, <https://doi.org/10.1038/cdd.2017.186>, 1.
- [2] I. Kapoor, J. Bodo, B.T. Hill, E.D. Hsi, A. Almasan, Targeting BCL-2 in B-cell malignancies and overcoming therapeutic resistance, in: *Cell Death and Disease*, vol. 11, Springer Nature, Nov. 01, 2020, <https://doi.org/10.1038/s41419-020-03144-y>, 11.
- [3] K.A. Sarosiek, A. Letai, Directly targeting the mitochondrial pathway of apoptosis for cancer therapy using BH3 mimetics – recent successes, current challenges and future promise, in: *FEBS Journal*, Blackwell Publishing Ltd, Oct. 01, 2016, pp. 3523–3533, <https://doi.org/10.1111/febs.13714>.
- [4] K.A. Sarosiek, T. Ni Chonghaile, A. Letai, Mitochondria: gatekeepers of response to chemotherapy, *Trends Cell Biol.* 23 (12) (Dec. 2013) 612–619, <https://doi.org/10.1016/j.tcb.2013.08.003>.
- [5] S. Fulda, K.M. Debatin, Extrinsic versus intrinsic apoptosis pathways in anticancer chemotherapy, *Oncogene* 25 (34) (Aug. 07, 2006) 4798–4811, <https://doi.org/10.1038/sj.onc.1209608>.

- [6] K.L. O'Neill, K. Huang, J. Zhang, Y. Chen, X. Luo, Inactivation of prosurvival Bcl-2 proteins activates Bax/Bak through the outer mitochondrial membrane, *Genes Dev.* 30 (8) (Apr. 2016) 973–988, <https://doi.org/10.1101/gad.276725.115>.
- [7] M.H. Kang, C.P. Reynolds, Bcl-2 Inhibitors: targeting mitochondrial apoptotic pathways in cancer therapy, *Clin. Cancer Res.* 15 (4) (Feb. 2009) 1126–1132, <https://doi.org/10.1158/1078-0432.CCR-08-0144>.
- [8] C.L. Hann, et al., Therapeutic efficacy of ABT-737, a selective inhibitor of BCL-2, in small cell lung cancer, *Cancer Res.* 68 (7) (Apr. 2008) 2321–2328, <https://doi.org/10.1158/0008-5472.CAN-07-5031>.
- [9] M.P. Kline, et al., ABT-737, an inhibitor of Bcl-2 family proteins, is a potent inducer of apoptosis in multiple myeloma cells, *Leukemia* 21 (7) (2007) 1549–1560, <https://doi.org/10.1038/sj.leu.2404719>.
- [10] T. Oltersdorf, et al., An inhibitor of Bcl-2 family proteins induces regression of solid tumours, *Nature* 435 (7042) (Jun. 2005) 677–681, <https://doi.org/10.1038/nature03579>.
- [11] E. Hwang, et al., ABT-737 ameliorates docetaxel resistance in triple negative breast cancer cell line, *Ann Surg Treat Res* 95 (5) (Nov. 2018) 240–248, <https://doi.org/10.4174/ast.2018.95.5.240>.
- [12] O. Kutuk, A. Letai, Alteration of the mitochondrial apoptotic pathway is key to acquired paclitaxel resistance and can be reversed by ABT-737, *Cancer Res.* 68 (19) (Oct. 2008) 7985, <https://doi.org/10.1158/0008-5472.CAN-08-1418>. –7994.
- [13] M. Broecker-Preuss, N. Becher-Boveleth, S. Müller, K. Mann, The BH3 mimetic drug ABT-737 induces apoptosis and acts synergistically with chemotherapeutic drugs in thyroid carcinoma cells, *Cancer Cell Int.* 16 (1) (Apr. 2016), <https://doi.org/10.1186/s12935-016-0303-8>.
- [14] V.D.G. Moore, J.R. Brown, M. Certo, T.M. Love, C.D. Novina, A. Letai, Chronic lymphocytic leukemia requires BCL2 to sequester prodeath BIM, explaining sensitivity to BCL2 antagonist ABT-737, *J. Clin. Invest.* 117 (1) (Jan. 2007) 112–121, <https://doi.org/10.1172/JCI28281>.
- [15] J.L. Mott, G.J. Gores, Piercing the armor of hepatobiliary cancer: Bcl-2 homology domain 3 (BH3) mimetics and cell death, *Hepatology* 46 (3) (Sep. 2007) 906–911, <https://doi.org/10.1002/hep.21812>.
- [16] C. Tse, et al., ABT-263: a potent and orally bioavailable Bcl-2 family inhibitor, *Cancer Res.* 68 (9) (May 2008) 3421–3428, <https://doi.org/10.1158/0008-5472.CAN-07-5836>.
- [17] K. Cho, X. Wang, S. Nie, Z. Chen, D.M. Shin, Therapeutic nanoparticles for drug delivery in cancer, *Clin. Cancer Res.* 14 (5) (Mar. 01, 2008) 1310–1316, <https://doi.org/10.1158/1078-0432.CCR-07-1441>.
- [18] M.J. Mitchell, M.M. Billingsley, R.M. Haley, M.E. Wechsler, N.A. Peppas, R. Langer, Engineering precision nanoparticles for drug delivery, in: *Nature Reviews Drug Discovery*, vol. 20, Nature Research, Feb. 01, 2021, pp. 101–124, <https://doi.org/10.1038/s41573-020-0090-8>, 2.
- [19] D. Kalyane, N. Raval, R. Maheshwari, V. Tambe, K. Kalia, R.K. Tekade, Employment of enhanced permeability and retention effect (EPR): nanoparticle-based precision tools for targeting of therapeutic and diagnostic agent in cancer, in: *Materials Science and Engineering C*, vol. 98, Elsevier Ltd, May 01, 2019, pp. 1252–1276, <https://doi.org/10.1016/j.msec.2019.01.066>.
- [20] J. Wu, The enhanced permeability and retention (EPR) effect: the significance of the concept and methods to enhance its application, in: *Journal of Personalized Medicine*, vol. 11, MDPI, Aug. 01, 2021, <https://doi.org/10.3390/jpm11080771>, 8.
- [21] S. Sindhvani, et al., The entry of nanoparticles into solid tumours, *Nat. Mater.* 19 (5) (May 2020) 566–575, <https://doi.org/10.1038/s41563-019-0566-2>.
- [22] P. Baluk, H. Hashizume, D.M. McDonald, Cellular abnormalities of blood vessels as targets in cancer, *Curr. Opin. Genet. Dev.* 15 (1) (Feb. 2005) 102–111, <https://doi.org/10.1016/j.gde.2004.12.005>.
- [23] Y. Nakamura, A. Mochida, P.L. Choyke, H. Kobayashi, Nanodrug delivery: is the enhanced permeability and retention effect sufficient for curing cancer?, in: *Bioconjugate Chemistry*, vol. 27 American Chemical Society, Oct. 19, 2016, pp. 2225–2238, <https://doi.org/10.1021/acs.bioconjchem.6b00437>, 10.
- [24] D. Schmid, et al., Nanoencapsulation of ABT-737 and camptothecin enhances their clinical potential through synergistic antitumor effects and reduction of systemic toxicity, *Cell Death Dis.* 5 (10) (Jan. 2014), <https://doi.org/10.1038/cddis.2014.413>.
- [25] D.M. Valcourt, M.N. Dang, M.A. Scully, E.S. Day, Nanoparticle-mediated Co-delivery of notch-1 antibodies and ABT-737 as a potent treatment strategy for triple-negative breast cancer, *ACS Nano* 14 (3) (Mar. 2020) 3378–3388, <https://doi.org/10.1021/acsnano.9b09263>.
- [26] N. Habibi, N. Kamaly, A. Memic, H. Shafiee, Self-assembled peptide-based nanostructures: smart nanomaterials toward targeted drug delivery, in: *Nano Today*, vol. 11, Elsevier B.V., Feb. 01, 2016, pp. 41–60, <https://doi.org/10.1016/j.nantod.2016.02.004>, 1.
- [27] M. Liu, X. Fang, Y. Yang, C. Wang, Peptide-enabled targeted delivery systems for therapeutic applications, in: *Frontiers in Bioengineering and Biotechnology*, vol. 9, Frontiers Media S.A., Jul. 01, 2021, <https://doi.org/10.3389/fbioe.2021.701504>.
- [28] R. Sharma, et al., Functionalized peptide-based nanoparticles for targeted cancer nanotherapeutics: a state-of-the-art review, in: *ACS Omega*, vol. 7, American Chemical Society, Oct. 18, 2022, pp. 36092–36107, <https://doi.org/10.1021/acsomega.2c03974>, 41.
- [29] W. jin Jeong, J. Bu, L.J. Kubiatowicz, S.S. Chen, Y.S. Kim, S. Hong, Peptide–nanoparticle conjugates: a next generation of diagnostic and therapeutic platforms?, in: *Nano Convergence*, vol. 5 Korea Nano Technology Research Society, Dec. 01, 2018 <https://doi.org/10.1186/s40580-018-0170-1>, 1.
- [30] C.P. Cerrato, K. Künnappu, Ü. Langel, Cell-penetrating peptides with intracellular organelle targeting, in: *Expert Opinion on Drug Delivery*, vol. 14, Taylor and Francis Ltd, Feb. 01, 2017, pp. 245–255, <https://doi.org/10.1080/17425247.2016.1213237>, 2.
- [31] C.P. Cerrato, Ü. Langel, An update on cell-penetrating peptides with intracellular organelle targeting, *Expert Opin Drug Deliv* 19 (2) (2022) 133–146, <https://doi.org/10.1080/17425247.2022.2034784>.
- [32] D. Juretić, Designed multifunctional peptides for intracellular targets, in: *Antibiotics*, vol. 11, MDPI, Sep. 01, 2022, <https://doi.org/10.3390/antibiotics11091196>, 9.
- [33] C. Ma, F. Xia, S.O. Kelley, Mitochondrial targeting of probes and therapeutics to the powerhouse of the cell, in: *Bioconjugate Chemistry*, vol. 31, Dec. 16, 2020, pp. 2650–2667, <https://doi.org/10.1021/acs.bioconjchem.0c00470>, 12. American Chemical Society.
- [34] I. Cohen-Erez, H. Rapaport, Coassemblies of the anionic polypeptide γ -PGA and cationic β -sheet peptides for drug delivery to mitochondria, *Biomacromolecules* 16 (12) (Dec. 2015) 3827–3835, <https://doi.org/10.1021/acs.biomac.5b01140>.
- [35] I. Cohen-Erez, H. Rapaport, Negatively charged polypeptide-peptide nanoparticles showing efficient drug delivery to the mitochondria, *Colloids Surf. B Biointerfaces* 162 (Feb. 2018) 186–192, <https://doi.org/10.1016/j.colsurfb.2017.11.048>.
- [36] I. Cohen-Erez, et al., Antitumor effect of lonidamine-polypeptide-peptide nanoparticles in breast cancer models, *ACS Appl. Mater. Interfaces* 11 (36) (Sep. 2019) 32670–32678, <https://doi.org/10.1021/acsmi.9b09886>.
- [37] N. Ben Ghedalia-Peled, I. Cohen-Erez, H. Rapaport, R. Vago, Aggressiveness of 4T1 breast cancer cells hampered by Wnt production-2 inhibitor nanoparticles: an in vitro study, *Int. J. Pharm.* 596 (Mar. 2021), <https://doi.org/10.1016/j.ijpharm.2021.120208>.
- [38] C. Charles, et al., Mitochondrial responses to organelle-specific drug delivering nanoparticles composed of polypeptide and peptide complexes, *Nanomedicine* 15 (30) (Dec. 2020) 2917–2932, <https://doi.org/10.2217/nmm-2020-0266>.
- [39] M.D. Sutherland, T.R. Kozel, Macrophage uptake, intracellular localization, and degradation of poly- γ -D-glutamic acid, the capsular antigen of *Bacillus anthracis*, *Infect. Immun.* 77 (1) (Jan. 2009) 532–538, <https://doi.org/10.1128/IAI.01009-08>.
- [40] B.D. Uleyr, L.S. Nair, C.T. Laurencin, Biomedical applications of biodegradable polymers, *J. Polym. Sci., Part B: Polym. Phys.* 49 (12) (Jun. 15, 2011) 832–864, <https://doi.org/10.1002/polb.22259>.
- [41] G. Yosefi, I. Cohen-Erez, E. Nativ-Roth, H. Rapaport, R. Bitton, Spontaneous alignment of self-assembled cationic and amphiphilic β -sheet peptides, *Adv. Mater. Interfac.* 7 (14) (Jul. 2020), <https://doi.org/10.1002/admi.202000332>.
- [42] G. Yosefi, T. Levi, H. Rapaport, R. Bitton, Time matters for macroscopic membranes formed by alginate and cationic β -sheet peptides, *Soft Matter* 16 (44) (Nov. 2020) 10132–10142, <https://doi.org/10.1039/d0sm01197e>.
- [43] Z. Azoulay, H. Rapaport, The assembly state and charge of amphiphilic β -sheet peptides affect blood clotting, *J. Mater. Chem. B* 4 (22) (2016) 3859–3867, <https://doi.org/10.1039/c6tb00330c>.
- [44] G. Yosefi, I. Cohen-Erez, E. Nativ-Roth, H. Rapaport, R. Bitton, Spontaneous alignment of self-assembled cationic and amphiphilic β -sheet peptides, *Adv. Mater. Interfac.* 7 (14) (Jul. 2020), <https://doi.org/10.1002/admi.202000332>.

- [45] T.P. Vinod, et al., Transparent, conductive, and SERS-active Au nanofiber films assembled on an amphiphilic peptide template, *Nanoscale* 5 (21) (Nov. 2013) 10487–10493, <https://doi.org/10.1039/c3nr03348a>.
- [46] I. Cohen-Erez, N. Harduf, H. Rapaport, Oligonucleotide loaded polypeptide-peptide nanoparticles towards mitochondrial-targeted delivery, *Polym. Adv. Technol.* 30 (10) (Oct. 2019) 2506–2514, <https://doi.org/10.1002/pat.4707>.
- [47] D. L. Nelson and M. M. Cox, 'Lehninger Principles of Biochemistry, fourth ed.'
- [48] S.T. Heller, T.P. Silverstein, pK a values in the undergraduate curriculum: introducing pK a values measured in DMSO to illustrate solvent effects, *ChemTexts* 6 (2) (Jun. 2020), <https://doi.org/10.1007/s40828-020-00112-z>.
- [49] S. Tshepelevitsh, et al., On the basicity of organic bases in different media, in: *European Journal of Organic Chemistry*, vol. 2019, Wiley-VCH Verlag, Oct. 31, 2019, pp. 6735–6748, <https://doi.org/10.1002/ejoc.201900956>, 40.
- [50] B.B. Touré, et al., The Role of the acidity of N-heteroaryl sulfonamides as inhibitors of Bcl-2 family protein-protein interactions, *ACS Med. Chem. Lett.* 4 (2) (Feb. 2013) 186–190, <https://doi.org/10.1021/ml300321d>.